Multistep laser excitation of barium: Apparent interferences due to overlap-integral variations

N. H. Tran, R. Kachru, and T. F. Gallagher
Molecular Physics Laboratory, SRI International, Menlo Park, California 94025
(Received 14 June 1982)

We report new, more extensive photoexcitation spectra of Ba autoionizing states which demonstrate that apparent interferences between discrete autoionizing states are in fact not interferences as previously proposed. A simple alternative interpretation of the "interference"-like line shapes as being due to variations in the spectral density of the autoionizing states and their overlap integrals with the bound initial state is presented and shown to agree with experiment. We argue that such spectra allow perhaps the most accurate determination of quantum defects, and should be a useful spectroscopic probe of autoionizing states.

One of the most familiar aspects in the study of atomic autoionizing states is the observation of interferences between excitation to these discrete states and excitation to the degenerate underlying continuum. The resulting asymmetric structures, known as Beutler-Fano profiles,[1] are routinely seen in UV photoabsorption spectroscopy of autoionizing states,[2] and in fact until recently all observations of autoionizing states were in the form of Beutler-Fano profiles. The development of multistep laser excitation[3] has made it possible to excite autoionizing states in such a manner that the continuum excitation is suppressed, so that only the discrete states are excited. One can then observe directly the discrete autoionizing state without any interference from the underlying continuum. In fact with low power laser excitation the autoionizing state is manifested as an approximately Lorentzian line whose energy and width are easily determined. At high laser powers, apparent interference features in the wings of the state under study are observed which correspond to higher and lower members of the same series.[4] These apparent interferences were previously attributed to the interference between excitation of the higher and lower series members and the power-broadened wing of the state under study.[4] More extensive observations have led us to conclude that the agreement between the observed spectrum and that calculated with the procedure mentioned above was fortuitous. This has led us to formulate the problem in a more general way which shows that the apparent interferences do not arise from interferences at all but from the variations of spectral densities and overlap integrals. Here we present the results of recent experiments with Ba $6p_jns$ and $6p_jnd$ states, outline the essence of the theoretical approach, and compare the experimental and calculated spectra.

The experimental setup has been described elsewhere.[5] Briefly, it consists of a barium atomic beam (density $\sim 10^8$ atoms/cm^3) crossed at right angles by three nearly collinear pulsed dye-laser beams. The first laser drives the $6s^2 \rightarrow 6s6p$ resonance transition in Ba, the second laser subsequently excites the $6s6p$ atoms to a bound Rydberg $6sn_0l$ state ($l=0$ or 2), and the third laser is scanned through the transitions $6sn_0l \rightarrow 6p_{1/2}nl$ or $6p_{3/2}nl$, that is, the $6s$ core electron is excited to a $6p_{1/2}$ or $6p_{3/2}$ state, while the Rydberg n_0s or n_0d electron makes a slight readjustment of its orbit to an ns or nd state, respectively. Immediately after the laser pulses, a small electric field is applied to sweep the ions produced by autoionization of the $6p_jnl$ states into an electron multiplier, the output of which is fed into a boxcar averager and then into a PDP11/03 digital computer for signal averaging and subsequent analysis. As the third laser is scanned, the computer also records its power, as well as its transmission through a 3.52-cm^{-1} free-spectral-range etalon to record the laser wavelength.

In the excitation of the autoionizing $6p_jnl$ state from the bound $6sn_0l$ state by the third laser, it is also possible that one-electron photoionization of the $6s\epsilon l \pm 1$ continua occurs, but the photoionization cross section of an $n \sim 15$ bound Rydberg state by a visible photon is vanishingly small, $\sim 10^{-20}$ cm^2. Similarly the two-electron photoionization to the $5d_{3/2,5/2}$ (and $6p_{1/2}$ when available) continua is observed to be weak (though this is not necessarily always true). On the other hand, excitation to the autoionizing $6p_jnl$ state has the oscillator strength $f \simeq 1$ of the Ba^+ resonance line spread over a few wave numbers leading to a photoexcitation cross section of $\sim 10^{-14}$ cm^2. Thus at low powers of the third laser we observe only the transitions $6sn_0l \rightarrow 6p_jnl$ with $n \simeq n_0$, giving rise to approximately Lorentzian lines. However at higher powers we observe spectra such as the one shown in Fig. 1, where the third laser is swept from 21 535 to 22 329 cm^{-1}, which energetically allows the excitation of $6p_{3/2}13d$ to $6p_{3/2}20d$ states from the bound $6s15d\,^1D_2$ state. The broad central peak in Fig. 1 corresponds to the main $6s15d\,^1D_2$

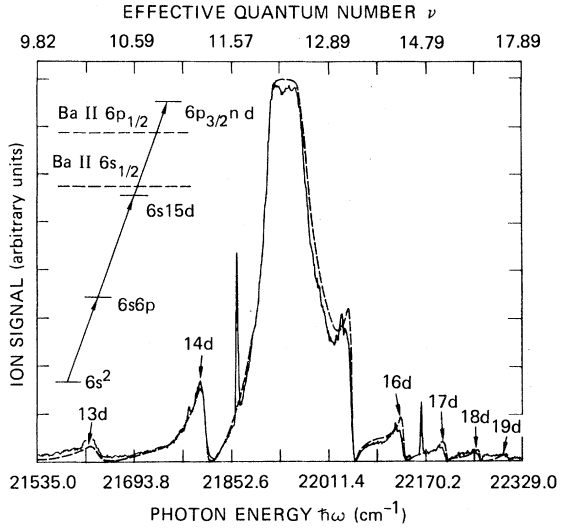

FIG. 1. Photoexcitation spectrum of the $6s15d\,^1D_2 \rightarrow (6p_{3/2}nd)_{J=3}$ transitions in Ba. The broken line is the spectrum calculated from Eqs. (2) and (4). The correspondence between ν and $\hbar\omega$ is given by Eq. (3). The energy level inset is not to scale.

$\rightarrow (6p_{3/2}15d)_{J=3}$ transition[6] in Ba at 21 942 cm^{-1}. (By circularly polarizing the three lasers in the same sense we ensure that only $J=3$ is populated.) The sharp feature at 21 861.9 cm^{-1} is due to two-photon ionization from the $6s6p$ state via the $6s10d\,^3D_2$ level[6] by the third laser. Together with the fringes transmitted through the 3.52-cm^{-1} etalon, this frequency marker enables us to determine the energy scale (abscissa) in Fig. 1 to an accuracy of $\sim$1 cm^{-1}. The ordinate scale is proportional to the number of ions produced by autoionization. The interferencelike structures correspond to the $6p_{3/2}nd$ states ($n=13,14,16,17$, etc.) as indicated in Fig. 1.

The apparently complicated spectrum of Fig. 1 can be understood by using a straightforward two-channel treatment[7] which is outlined here and will be presented in more detail later. The two channels are the $6p_{3/2}nd$ closed channel and a continuum. All continua are lumped together since excitation to the continuum is negligible and the continuum serves only as a decay channel for the autoionizing atoms. With no continuum excitation the spectrum of Fig. 1 must be due entirely to excitation of the $(6p_{3/2}nd)_{J=3}$ channel. The wave function for this channel is given by

$$|6pnd\rangle = \Phi Z(\nu)v(\nu,d) \quad . \tag{1}$$

Here Φ contains the wave function for the $6p$ electron and the spin and angular parts of the νd electron, the effective quantum number ν of the autoionizing $6p_{3/2}nd$ channel is a *continuous* variable defined by the fact that $v(\nu,d)$ is a Coulomb radial wave function for a d electron of binding energy $\mathcal{R}/\nu^2$ ($\mathcal{R}$ being Rydberg's constant), and $Z^2(\nu)$, the spectral density of the $6p_{3/2}nd$ channel [see Eq. (42) of Ref. 7], can be calculated using two-channel quantum defect theory[7] from the known $6p_{3/2}nd$ quantum defect[8] $\delta=2.75$, and autoionization widths[8] $\Gamma_n=0.23\nu^{-3}\mathcal{R}$. [$Z^2(\nu)$ is proportional to the slope of the Lu-Fano plot of these channels.[7]]

The cross section for photoexcitation σ is proportional to the transition matrix element squared $|a_n|^2 = |\langle 6s15d|\mu|6pnd\rangle|^2$ (μ is the electric dipole operator). Since the $6s15d \rightarrow 6pnd$ transition may be viewed as the $6s \rightarrow 6p$ transition of Ba^+ with the outer Rydberg electron making the requisite adjustment in its orbit we may factor the matrix element a_n into a Ba^+ dipole matrix element and an overlap integral which is obtained using the wave function of Eq. (1).

$$\sigma \propto |a_n|^2 \propto |\langle 6s|\mu|6p\rangle|^2 Z^2(\nu) |\langle 15d|v(\nu,d)\rangle|^2 \quad . \tag{2}$$

The physical significance of the factors in Eq. (2) is easily appreciated. The Ba^+ dipole matrix element is a constant which we may ignore. In Fig. 2(a) we plot the spectral density $Z^2(\nu)$, a periodic function of ν peaking at the locations $\nu = n-\delta = n-2.75$ of the $6p_{3/2}nd$ autoionizing states whose energies $W(6p_{3/2}nd)$ are given by

$$W(6p_{3/2}nd) = W(6s15d) + \hbar\omega = V_{IP}(6p_{3/2}) - \mathcal{R}/\nu^2 \quad , \tag{3}$$

where $V_{IP}(6p_{3/2})$ is the ionization potential to the $Ba^+6p_{3/2}$ state, and ω is the angular frequency of the (third laser) photon driving the transitions $6s15d \rightarrow 6p_{3/2}nd$.

The overlap integral squared $|\langle 15d|v(\nu,d)\rangle|^2$ is plotted in Fig. 2(b). Note that it is equal to $|\langle 15d|nd\rangle|^2\nu^3$ where $|nd\rangle$ has the usual bound state normalization $\langle nd|nd\rangle = 1$. The effective quantum number of the $6s15d$ state is[6] $n_0^* = 12.35$ ($\delta_0 = 2.65$), thus the overlap integral $|\langle 15d|v(\nu,d)\rangle|^2 = (1)\ \nu^3$ for $\nu = 12.35$ and vanishes for $\nu = 12.35 \pm i$ for positive integers i due to the orthogonality of the Coulomb wave functions. Finally Fig. 2(c) shows the photoexcitation cross section which is proportional to the product of the spectral density and overlap integral squared.

Since the overlap integral $|\langle 15d|v(\nu,d)\rangle|^2(\nu)$ decreases rapidly away from the main $6s15d \rightarrow 6p15d$ transition [see Fig. 2(b)], the cross section $\sigma(\nu)$ is roughly 500 times larger on the main transition than on subsequent peaks, as shown in Fig. 2(c). Consequently, in order to have a significant ($\sim$10%) probability of driving the subsidiary $6s15d \rightarrow 6pnd$ ($n \neq 15$) transitions, one necessarily has a probability of 1 of driving the main $6s15d \rightarrow 6p15d$ transition, in the vicinity of which the ion signal will obviously not be linear in the laser power. This "depletion broadening" mechanism[9] causes the observed ion signal to

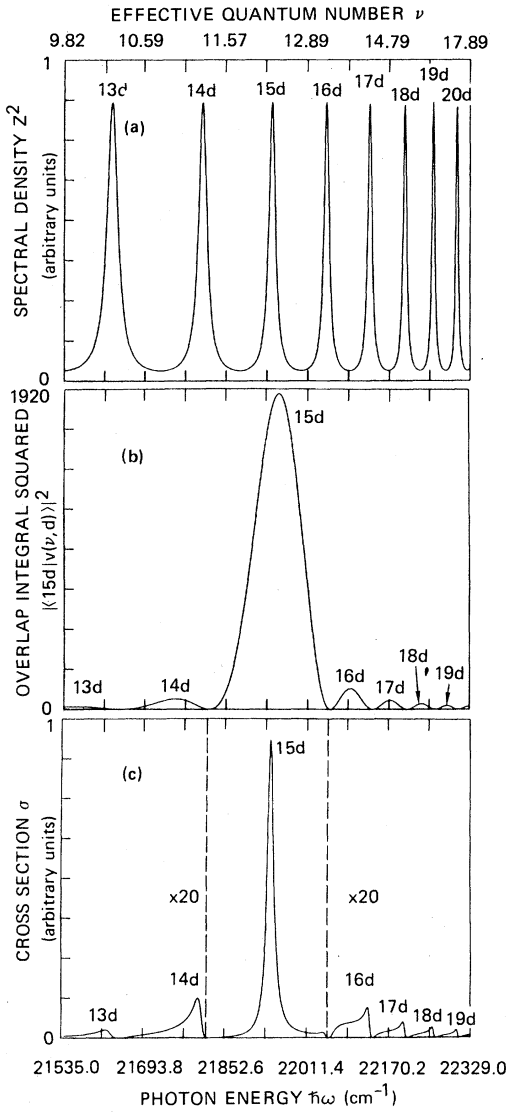

FIG. 2. Spectral density, overlap integral, and photoexcitation cross section for the spectrum of Fig. 1. Note the change in scale (×20) in the wings of (c).

vary as

$$s(\nu) \propto 1 - e^{-\sigma(\nu)\phi(\nu)} , \tag{4}$$

where $\phi(\nu)$ is the incident photon flux. In Fig. 1 we plot $s(\nu)$ given by Eq. (4) with the cross section $\sigma(\nu)$ calculated in Fig. 2(c) and the laser flux $\phi(\nu)$ measured concurrently with the ion signal, as described earlier. [Note that at the central feature of Fig. 1 the product $\sigma(\nu)\phi(\nu)$ is ~100.] We believe that the slight discrepancy between the experimental and theoretical spectra is due to uncertainties (~1 cm^{-1}) in the wavelength scale and fluctuations (~30% peak to peak) in the laser power, as well as our two-channel treatment which cannot account for variations (~0.02[8]) in the quantum defects δ and departures ($\lesssim$20%[8]) from the ν^{-3} scaling law for the autoionizing width Γ_n, as n varies from 13 to 20.

We should point out two features implied by this treatment. First, note that since the asymmetric profiles arise from the product spectral density times overlap integral, the shape of the spectra is an extremely sensitive function of both the quantum defect difference $\Delta \equiv \delta - \delta_0$ and the autoionizing widths Γ_n. In particular, the sign of the asymmetry is expected to reverse as Δ changes sign, as indeed happens with the $6s18s \rightarrow 6p_{1/2}ns$ transitions (Fig. 3), for which $\Delta<0$, whereas it is >0 for the spectrum of Fig. 1.

Second, this treatment implies that a zero will always be observed in the excitation spectrum whenever $\nu = n_0^* \pm i$, even in the case $\Delta = 0$ [see Fig. 2(b)]. This is in direct contrast to the interference model suggested previously,[4] which predicted that in the case $\Delta = 0$ the transition amplitude to the subsidiary peak would vanish leaving the wing of the central feature undisturbed. In fact we always observe a zero in the excitation spectrum at the locations corresponding to $\nu = n_0^* \pm i$, as shown in Figs. 1 and 3, even for the case[10] $\Delta = 0$, in accord with the model discussed here, but in contradiction to the previously presented interference model.

With a two-channel quantum defect analysis on the spectrum of Fig. 3, we have been able to model the experimental line shape to an accuracy of only about 10% over the whole range shown in Fig. 3. This is not surprising since such an analysis is not expected to account for perturbed Rydberg series such as the $6p_{1/2}ns$ series of Fig. 3. Preliminary measurements by Cooke and co-workers[11] suggest quantum defect variations of up to ~0.1 and departures from the ν^{-3} behavior of the autoionizing widths Γ_n of up to ~50% as n goes from 16 to 21. A three-channel analysis is being undertaken on the data of Fig. 3 and other similar spectra,[10] which should yield very accu-

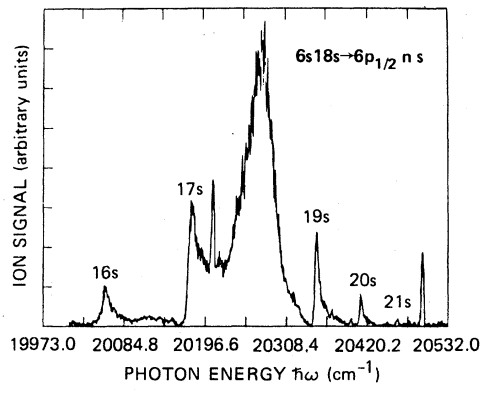

FIG. 3. Photoexcitation spectrum of the $6s18s \rightarrow 6p_{1/2}ns$ transitions in Ba.

rate values for the quantum defects of these autoionizing states in Ba, since the exact spectral line shape is very sensitive to these values, as can be seen from Figs. 1 and 3. Furthermore, one can also take advantage of this sensitivity of the spectral line shape to probe configuration interactions between different Rydberg series, and indeed we have already obtained[10] experimental spectra that clearly show configuration interaction effects between various Rydberg channels in barium.

In summary, we have presented new experimental evidence showing that excitation spectra which apparently exhibit interference between excitations to different *discrete* Rydberg states are in fact due to variations in the spectral density of autoionizing states and their overlap integrals with the bound initial state. This new understanding, together with new experimental data that show extremely strong dependence on the values of quantum defects and autoionizing linewidths, should provide a novel and convenient probe for series perturbation and configuration interaction in highly excited atoms.

It is a pleasure to acknowledge fruitful discussions with K. A. Safinya, W. E. Cooke, D. L. Huestis, and U. Fano in the course of this work, which was supported by the National Science Foundation under Grant No. PHY 800-70041.

[1]U. Fano, Phys. Rev. 124, 1866 (1961).
[2]W. R. S. Garton and K. Codling, Proc. Phys. Soc. London 75, 87 (1960), for example.
[3]W. E. Cooke, T. F. Gallagher, S. A. Edelstein, and R. M. Hill, Phys. Rev. Lett. 40, 178 (1978).
[4]K. A. Safinya and T. F. Gallagher, Phys. Rev. Lett. 43, 1239 (1979).
[5]T. F. Gallagher, L. M. Humphrey, W. E. Cooke, R. M. Hill, and S. A. Edelstein, Phys. Rev. A 16, 1098 (1977).
[6]J. R. Rubbmark, S. A. Borgström, and K. Bockasten, J. Phys. B 10, 421 (1977).
[7]U. Fano, Phys. Rev. A 2, 353 (1970).
[8]F. Gounand, T. F. Gallagher, W. Sandner, K. A. Safinya, and R. Kachru (unpublished).
[9]W. E. Cooke, S. A. Bhatti, and C. L. Cromer, Opt. Lett. 7, 69 (1982).
[10]N. H. Tran, T. F. Gallagher, and R. Kachru (unpublished).
[11]W. E. Cooke *et al.* (unpublished).